

PAPER • OPEN ACCESS

High performance emission spectrometer at Balder/MAX IV beamline

To cite this article: K Klementiev *et al* 2016 *J. Phys.: Conf. Ser.* **712** 012018

View the [article online](#) for updates and enhancements.

You may also like

- [Self-normalized photoacoustic technique for measurement of thermal diffusivity for metals](#)
J A Balderas-López
- [The isoelectronic trap iodine in AgBr](#)
W Czaja and A Baldereschi
- [Semiempirical self-energy corrections to LDA bands of semiconductors, and a scaling law for the scissor operator](#)
V Fiorentini and A Baldereschi



ECS
The
Electrochemical
Society
Advancing solid state &
electrochemical science & technology

DISCOVER
how sustainability
intersects with
electrochemistry & solid
state science research

High performance emission spectrometer at Balder/MAX IV beamline

K Klementiev, I Preda, S Carlson, K Sigfridsson and K Norén

MAX IV Laboratory, 22363 Lund, Sweden

E-mail: konstantin.klementiev@maxlab.lu.se

Abstract. The emission spectrometer at Balder/MAX IV beamline is presented. Its unique features are described. Comparison is given with other types of curved crystals analyzers.

1. Introduction

Balder is a hard x-ray XAFS beamline at the brand new Swedish synchrotron MAX IV. It was designed for a broad energy range (2.4 – ~50 keV), high flux ($> 10^{13}$ ph/s), quick scanning (> 1 Hz repetition rate for full EXAFS [Extended X-ray Absorption Fine Structure]) and simultaneous high-resolution emission detection compatible with various sample set-ups [1].

High flux beamlines frequently experience overload problems in detecting fluorescence signals. Even with the last generation of signal processors, solid state detectors can hardly handle high count rates of > 1 Mcps/element. The repetition rate of spectra is thus limited by detectors, not by the primary flux. On the other hand, high energy resolution XES [X-ray Emission Spectroscopy] paves the way towards *site-selective* XAFS [X-ray Absorption Fine Structure] — disentangled spectra of individual species in a mixture. In such applications, high incoming flux is necessary to detect weak satellite lines and/or to work with low elemental concentrations. Balder will use its high flux source for XES but will have to tackle the overload problem.

In the next section we show that both tasks, high flux fluorescence detection and high resolution emission spectroscopy, can be solved with one instrument. The following sections describe the spectrometer at Balder beamline with focusing at its most crucial components — the crystals.

2. Comparison of 1D-bent crystal analyzers

In this section we compare Rowland circle based spectrometers utilizing simply bent (Johann [2]) and ground-bent (Johansson [3]) crystals and a von Hamos spectrometer [4]. The schematics of the three spectrometers can be found on the web page of xrt program [5] and are briefly outlined as follows. The Johann crystal is simply bent from a flat crystal to a cylinder of radius $2R$; the Johansson crystal is first cylindrically ground to a radius $2R$ and then bent down to a radius R . In both cases, the source (sample), the crystal and the detector lie on a circle (Rowland circle) of radius R . The grinding and/or bending occurs in the plane of the circle. The von Hamos crystal has *sagittal* bending, being flat in the diffraction plane. When a Johann crystal is rotated by 90° around the sample-to-crystal line, it becomes a von Hamos crystal that has to be put at a correct distance. This case is labeled as “Johann as von Hamos” and has a larger bending radius and thus a larger working distance than the other von Hamos crystals compared in this study. The Johann and Johansson crystals are 100(meridional)×20(sagittal) mm² with the



Rowland circle diameter 1 m. The von Hamos crystals are 100(sagittal)×50(meridional) mm² with the sagittal radius 250 mm, diced and continuously bent. All the crystals are Si(444).

The ray tracing study was done with the program xrt [5]. The resulted beam “images” are reported on the program's web page; here we only summarize the end results — energy resolution and efficiency.

In comparing with a von Hamos spectrometer, one should realize its strongest advantage — inherent energy dispersive operation without a need for energy scan. This advantage is especially important for broad emission lines. Below, the comparison is made for two cases: (1) a narrow energy band (figure 1, left), which is more interesting for valence band RIXS and which assumes a high resolution monochromator in the primary beam and (2) a wide energy band (figure 1, right), which is more interesting for core state RIXS and normal fluorescence detection. The desired position on the charts is in the upper left corner. As seen in the figures, the efficiency of the von Hamos crystals (i) is independent of the energy band (equal for the left and right charts), which demonstrates truly energy-dispersive behavior of the crystals but (ii) is significantly lower as compared to the Johann and Johansson crystals. A way to increase efficiency is to place the crystal closer to the source, which obviously decreases energy resolution because of the increased angular source size. Inversely, if the crystal is put at a further distance, the energy resolution is improved (see the von Hamos case with larger radius and distance, “Johann as von Hamos”, square symbols) but the efficiency is low because of a smaller solid angle collected.

Finally, among the compared 1D-bent spectrometers the Johansson type is the best in the combination of good energy resolution and high efficiency and therefore it can function both as a high resolution spectrometer and a fluorescence detector. One should bear in mind, however, two very strong advantages of von Hamos spectrometers: (1) they do not need alignment: a crystal and a detector positioned approximately will probably immediately work and (2) the image is inherently energy dispersive with a flat (energy independent) detector response. The low efficiency and mediocre energy resolution are a price for the alignment-free energy dispersive operation. Rowland circle based spectrometers will always require good alignment.

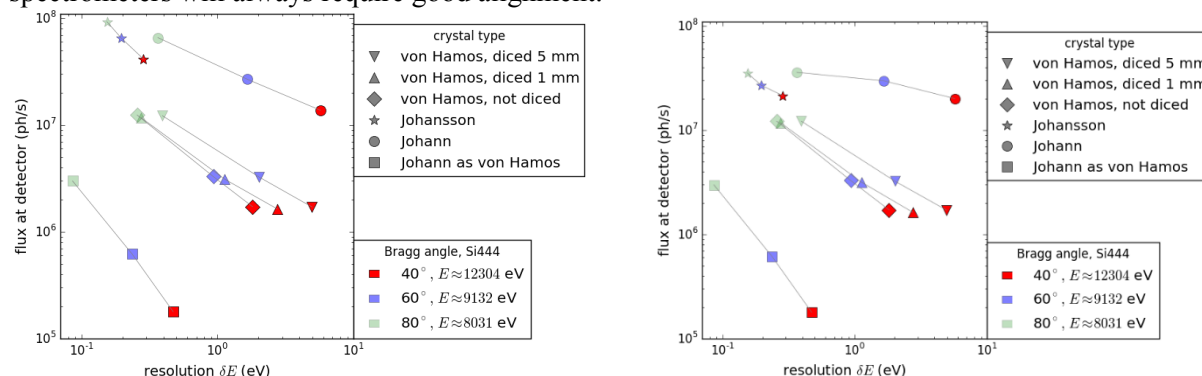


Figure 1. Resolution-efficiency charts of 1D-bent Si444 crystal analyzers at 10^{13} ph/s incoming flux and $100 \times 100 \mu\text{m}^2$ source size. The left chart is with a narrow source energy band equal to the 6-fold energy resolution; the right one is with a wide energy band equal to $8 \cdot 10^{-4} \cdot E$ (approx. width of $K \beta$ lines [6]).

3. Spectrometer design

The main design objectives are: 1) to be compatible with set-ups used for transmission XAFS detection in order to eliminate the need for a large *ad hoc* fluorescence window, 2) to have the emission energy axis dispersive, i.e. recorded without scanning, 3) to implement 2D detection for quicker and more visual alignment, 4) to serve both as a high resolution spectrometer and a standard fluorescence detector and 5) to leave ample space around the sample, also above it, for bulky sample holders as a cryostat or an in-situ chemical cell.

These objectives will be achieved by the back-scattering escape direction – not the usual 90° , variable in-Rowland-circle position – by the translation of the spectrometer towards the sample, large 2D pixel detectors, large ground-bent crystals and the detector stage *under* the sample position.

The overall design of the Balder end station, including the spectrometer, is sketched in figure 2. The crystals of $300 \times 40 \text{ mm}^2$ size are grouped in two branches, tunable for two, possibly different energies. The primary beam passes between the two branches. Two 2D detectors (one of them is under the table and not visible in figure 2) are coupled to the two crystal branches. The detectors are outside the vessel, behind a large curved window. The beam height at the end station enables a Rowland circle of $\sim 1.5 \text{ m}$ diameter. A light-weight removable vessel (several Viton-sealed covers) will be added at a later stage.

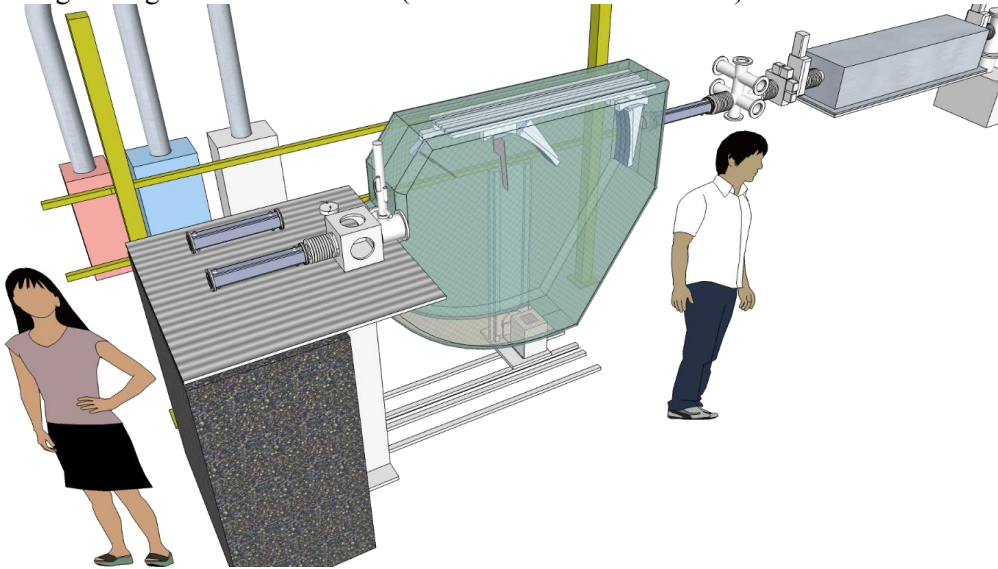


Figure 2. Balder end station. The monochromatic beam enters from the right. Shown are, in downstream direction, a vessel with harmonic rejecting mirrors (one of them will additionally focalize in vertical), beam conditioning and diagnostics elements, the spectrometer (with the semitransparent vessel), an adjustable table with two switchable experiments and a gas distribution system with various gas types (behind the table).

4. Crystals

The central part of the spectrometer – several crystals of various orientations – will be manufactured in-house. This project includes grinding, lapping, polishing, metrology measurements, special surface treatment, bending, assembling and testing with x-rays. The crystals will be of the Johansson type, i.e. ground to a radius equal to the Rowland circle diameter and bent down to one half of this radius. In order to bend a crystal, it has to be sufficiently thin. A safe thickness-to-radius ratio for silicon crystals is usually taken as 5000. We therefore aim at a thickness of $\sim 300 \mu\text{m}$.

We have established a silicon processing workshop at MAX IV Laboratory. For a test ground and polished crystal, so far not bent, we have achieved a high radius precision $R = 1503.6 \pm 0.6 \text{ mm}$. The resulted silicon arc is shown in figure 3.

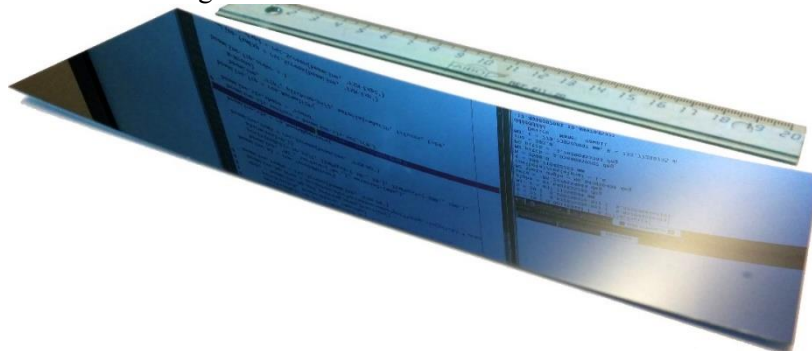


Figure 3. A ground and polished test silicon crystal. Notice that this is not a bent piece; the crystal planes are still flat and parallel to the table.

The next processing stage is the surface treatment. The amorphized surface layer is usually removed by chemical etching. Having the crystal thin and large, we believe a safer and more determined way is to subject the crystal to recrystallization in an ultra-high vacuum oven. A small test piece has exhibited re-appearance of a LEED pattern measured *in situ* in the oven. We are building a larger volume oven, also with an *in situ* LEED instrument, to work on the production crystals.

Meanwhile, the first batch of six Si(110) 310-mm-long crystals has been cut and ground (not lapped yet) to the radius 1500 mm, see figure 4.

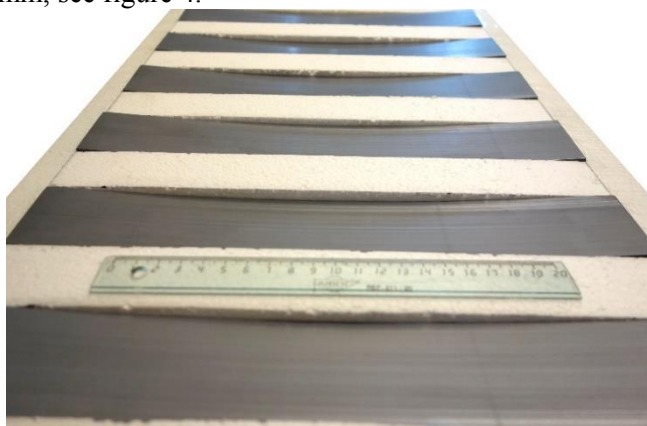


Figure 4. The first production batch of crystal analyzers. The upper surface is ground to 1.5 m radius.

5. Outlook

The spectrometer will be implemented in stages, starting with a smaller number of branches and crystal types and limited to a moderate energy range. Later on a lightweight vacuum chamber and a specialized low-energy detector will enable the usage of the spectrometer at low energies. A 2D on-the-fly image analysis will be developed for converting detector images into XES spectra.

The mechanical design is in progress. The spectrometer is planned for the first tests by end 2016.

6. Conclusion

Among various curved crystal analyzers, the Johansson type is the best in the combination of good energy resolution and high efficiency. This property is due to the exact point-to-point imaging provided by each point of the crystal along the Rowland circle. The future spectrometer at the Balder beamline is therefore selected to be of the Johansson type.

The back scattering (relatively to the sample) geometry makes the usual side windows in a cryostat or an *in situ* cell unnecessary and requires only the entrance window.

Large ground-bent crystals are being produced at the MAX IV Laboratory. The test pieces have demonstrated maturity of the developed technological steps.

Acknowledgments

The Balder beamline is funded by the Knut and Alice Wallenberg Foundation and Swedish universities.

References

- [1] Klementiev K, Norén K, Carlson S, Sigfridsson Clauss K and Persson I 2015 The BALDER Beamline at the MAX IV Laboratory, this volume
- [2] Johann H H 1931 *Z. Phys.* **69** 185–206
- [3] Johansson T 1933 *Z. Phys.* **82** 507–28
- [4] von Hámos L 1934 *Ann. Phys.* **411** 252–260
- [5] Klementiev K and Chernikov R 2014 Powerful scriptable ray tracing package xrt *Advances in Computational Methods for X-Ray Optics III* (Proc. SPIE 9209, 2014) ed Sanchez del Rio M and Chubar O 92090A pypi.python.org/pypi/xrt, pythonhosted.org/xrt
- [6] Henke B L, Gullikson E M and Davis J C 1993 *At. Data Nucl. Data Tables* **54** 181–342